

# Arrested Microphase Separation as a Route to Colloidal Gelation

P. Charbonneau<sup>1</sup> and D. R. Reichman<sup>2,\*</sup>

<sup>1</sup>*Chemistry and Chemical Biology, Harvard University, 12 Oxford Street, Cambridge, MA 02138*

<sup>2</sup>*Department of Chemistry, Columbia University, 3000 Broadway, New York, NY 10027*

(Dated: December 2, 2024)

In this letter we demonstrate the applicability of an augmented Gibbs ensemble Monte Carlo approach for the determination of the phase behavior of model colloidal systems with short-ranged depletion attractions and long-ranged repulsion. This technique allows for the first quantitative determination of the phase boundaries and ground states in such systems when the range of the attraction is a small fraction of the particle diameter. We demonstrate that gelation may occur in such systems as the result of arrested *microphase* separation, even when the equilibrium state of the system is characterized by compact microphase structures.

PACS numbers: 64.60.-i, 61.46.Bc, 61.20.Lc, 82.70.Dd, 82.70.Gg

Understanding the various routes to the formation of colloidal gels is a forefront problem in soft-condensed matter physics. It has been demonstrated via theory [1], experiment [2, 3], and simulation [4, 5] that a weak, porous solid may be formed when a suspension of colloidal particles with short-ranged depletion induced attractions is quenched below its critical point. Spinodal decomposition, expected to lead to complete phase separation into colloid-rich and colloid-poor regions, may arrest or become anomalously slow when bonding between colloidal particles is sufficiently strong. The resulting porous structure may support weak shear stresses, and is called a colloidal (or physical) gel. While equilibrium routes to physical colloidal gelation do exist [6, 7, 8], the non-equilibrium route described above is perhaps the most ubiquitous.

When excess charge resides on the colloidal particles, the situation is more complex [9]. In addition to short-ranged depletion interactions, the long-ranged repulsive portion of the potential may lead to the formation of various microphase structures, such as clusters, cylinders, sheets, and spirals [10, 11, 12, 13, 14]. As a result of charge frustration, the nature of physical gelation in such systems is potentially more subtle than in systems with attractive interactions alone. Indeed, several novel routes to gelation in such systems have been discussed. One such proposal is that compact, thermodynamically stable clusters may form the building blocks of a glassy state [15]. At high enough volume fraction clusters may aggregate or become caged as in the case for individual colloidal particles near the colloidal glass transition [16]. At low volume fractions, such a glassy state could be stabilized by the effective long-ranged repulsion between individual clusters [15]. More recently, it has been proposed that disordered or partially ordered anisotropic domains may be responsible for physical gelation in charged colloidal systems [11, 14, 17].

A major difficulty in testing the validity of any proposal resides in the accurate calculation of the phase diagram in systems with long-ranged repulsive and short-

ranged attractive interactions. When the range of the attractive interaction is comparable to the size of the particles, the phase behavior may be characterized easily even with standard simulation techniques [12, 13, 14]. On the other hand, when the attractive portion of the potential varies over distances that are a fraction of the particle size, sampling issues become severe, and direct molecular dynamics and Monte Carlo techniques are not feasible. Unfortunately is it in the short-ranged attractive limit that the gel phase is usually stabilized [4, 5]. We have recently demonstrated [18, 19] that a judicious implementation of the Gibbs ensemble Monte Carlo (GEMC) [20] technique allows for the computation of nearly complete phase behavior in systems with very short-ranged attractive interactions. In this letter we adapt the GEMC technique for the study of systems characterized by short-ranged strong attractions and long-ranged repulsion. The successful application of this approach provides crucial information on possible routes to gelation in systems with competing interactions. Indeed, our conclusions and interpretations of the mechanism of gelation differ from those previously drawn from studies of analogous systems.

In this work we study potentials of the form [15] [33]

$$U(r) = \left[ 4\epsilon \left( \left( \frac{\sigma}{r} \right)^{2n} - \left( \frac{\sigma}{r} \right)^n \right) + A \frac{e^{-r/\xi}}{r/\xi} \right]. \quad (1)$$

Large values of  $n$  correspond to increasingly shorter-ranged attractions. For visualization purposes, we focus on a two-dimensional system. As discussed below we expect all qualitative conclusions to be unmodified by this choice. Selected results will also be provided for the three-dimensional case. We study three-dimensional short-ranged attractive potentials ( $n = 50$ ) with Yukawa parameters ( $A = 0$ ;  $A = 1.275$  with  $\xi = 0.5$  and  $A = 0.203$  with  $\xi = 1$ ) and two-dimensional systems ( $n = 100$ ) with Yukawa parameters ( $A = 0$ ;  $A = 0.68$  with  $\xi = 1$ , and  $A = 0.2$  with  $\xi = 2$ ). For the last parameter set, the system is beyond the Lifshitz point (signaling the existence of microphase behavior in some

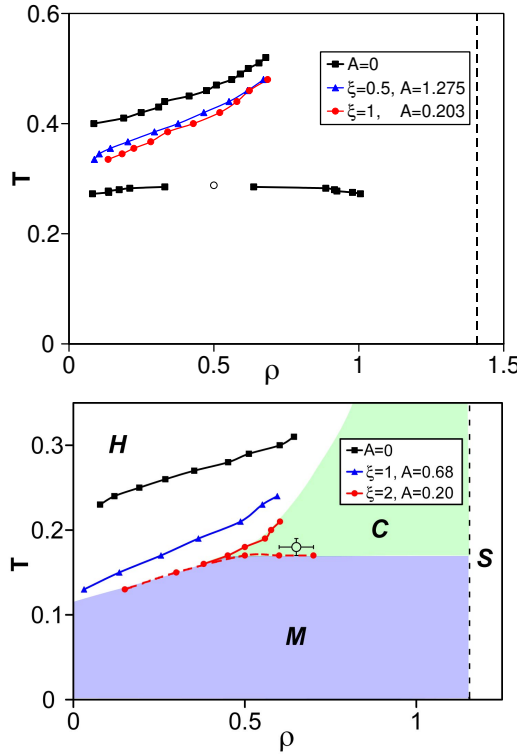


FIG. 1: Three-dimensional (top) and two-dimensional (bottom) phase diagrams for short-ranged attraction with an increasing range of repulsion, given by the screening parameter  $\xi$ . Lines are a guide to the eye only. GEMC gas-solid results and metastable gas-liquid are shown by solid lines. The short-dashed black line is the crystal close-packed density. The open circle represent the  $A = 0$  critical points in both top and bottom phase diagrams, as obtained by the extended corresponding states approach [21]. Uncertainty is smaller than the depicted dots except when otherwise indicated. Top:  $A = 0$  results are taken from earlier work [18]. Bottom: the long-dashed line is the microphase boundary for  $\xi = 2$  for which the uncertainty in  $T$  is  $\pm 0.01$ . Note that in the  $\xi = 2$  case the critical point exists only in the mean-field limit, and fluctuations render the microphase transition weakly first order.  $M$  denotes microphase regions,  $H$  denotes homogeneous phase,  $C$  denotes coexistence of gas and crystal, and  $S$  denotes solid.

region of the phase diagram) and a preliminary dynamical study for the three-dimensional version has been performed by Sciortino *et al* [15].

For the vapor-solid equilibrium, we have recently successfully implemented the GEMC methodology for short-ranged attractive systems [18]. For this region of the phase diagram, boxes are configured such that one box contains only vapor and the other a slab of solid surrounded by vapor [34]. Initial boxes contain 256 particles in the gas phase and 500 particles in the solid slab. A minimum of  $10^6$  Monte Carlo cycles are performed for equilibration and production. To characterize the phase behavior in the regime where microphase separa-

tion occurs, two identical boxes with a minimum of 256 particles on a lattice are used for initial configurations. At these lower temperatures, GEMC serves as an efficient phase space sampling algorithm somewhat akin in spirit to the grand canonical MC and parallel-tempering MC used in previous studies of systems with competing attractive and repulsive interactions [13]. It should be noted however that the approach implemented here is far more efficient at detecting complex phase boundaries. In particular, upon crossing from a gas-solid coexistence region to a microphase separated region, the sampling efficiency of parallel tempering MC would be dramatically reduced, even if standard non-local MC moves are introduced.

Before discussing the impact on phase equilibrium of the repulsive portion of the potential, we make some brief comments on the purely attractive case in two dimensions. The phase diagrams of short-ranged attractive two-dimensional systems have not been investigated as thoroughly as their three-dimensional counterparts. The existence of high density crystal-crystal coexistence in both two and three dimensions supports the notion that systems characterized by identical interactions in two and three dimensions are qualitatively similar [22]. While crystal-crystal coexistence does not occur in the temperature and density range of interest here, this phenomena is related to the metastability of the gas-liquid critical point, which does occur at densities and temperatures of concern in this work. With no repulsion ( $A = 0$ ), we thus expect the liquid-gas coexistence to become metastable for  $n \gtrsim 12$  and thus for  $n = 100$  we expect the gas-liquid binodal to be metastable and buried below the gas-solid coexistence line [23]. In three dimensions it is known that nucleation dynamics are dramatically influenced by this buried gas-liquid binodal [24, 25, 26]. Similar effects also appear in two dimensions, although metastable states are harder to observe, due to much faster nucleation. In the two-dimensional attractive case ( $A=0$ ), visual inspection of the relaxation dynamics accompanying apparent spinodal decomposition gives  $T_c = 0.18 \pm 0.01$ . This can be checked by combining the arguments developed by Noro and Frenkel regarding corresponding states for short-ranged potentials [21] with the location of the critical point coordinates extracted from the results of Seaton and Glandt for the Baxter limit of adhesive disks [27]. Such considerations yield a value identical to that found by visual inspection, while the critical density is found to be  $\rho_c = 0.6 \pm 0.1$ . For the same potential in three dimensions,  $T_c = 0.235 \pm 0.005$  [15] and  $\rho_c \sim 0.5$  [18, 28]. The metastable critical point is indicated in Fig. 1. The three-dimensional gas-solid coexistence curve is also reported in Fig. 1 for the range where GEMC simulations are possible.

We now turn to a discussion of the impact of repulsion on phase behavior. In three-dimensional systems with attractive ranges similar to that of  $n = 6$  LJ, the addi-

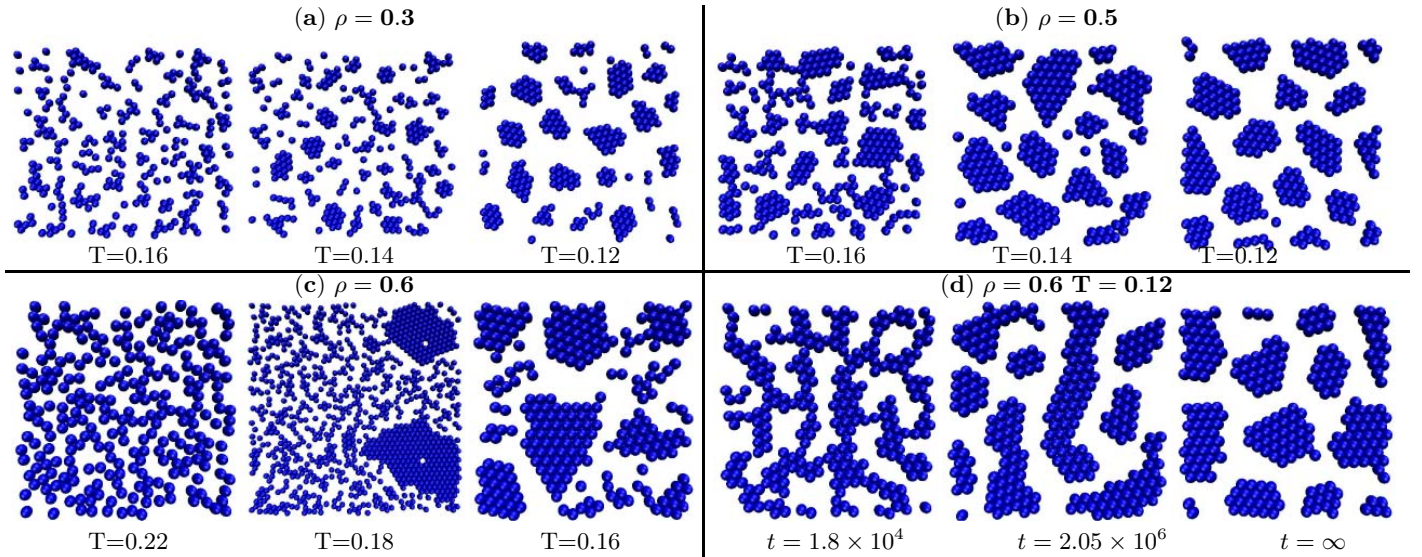


FIG. 2: Configurations for  $\xi = 2$  and  $A = 0.2$ . Thermodynamically equilibrated with GEMC at (a)  $\rho = 0.3$ , (b)  $\rho = 0.5$ , and (c)  $\rho = 0.6$  for the temperatures shown sequentially from left to right. (d) Evolution of a configuration under molecular dynamics at  $\rho = 0.6$  and  $T = 0.12$  (first two panels) and the final thermodynamic outcome determined via GEMC.

tion of small amplitude long-ranged repulsion is known to slightly depress the gas-liquid spinodal and binodal lines [29]. The addition of repulsion of either greater amplitude or longer range will transform the gas-liquid coexistence region into a microphase boundary where low and high density coexistence regions locally coexist. These effects may be seen in the phase diagram in the lower panel of Fig. 1. In particular, in the three-dimensional cases, adding repulsion destabilizes the crystal phase thereby extending the stability of the homogeneous phase to lower temperatures, as seen for the gas branch of the gas-crystal coexistence curve in Fig. 1. In the two-dimensional case for  $A = 0.2$  and  $\xi = 2$  where microphase separation occurs, the signature of this effect is the depression of the microphase boundary at low densities. In this case the high density phase is crystalline, since the microphase boundary is below the gas-solid coexistence line. GEMC temperature scans allow us to visually pinpoint the boundary of the microphase region. From the previous discussion, one expects the microphase boundary to be depressed with respect to the  $A = 0$  metastable critical point, and this is indeed observed. General arguments indicate that fluctuations alter the nature of the critical point, rendering the transition weakly first-order [30].

At this stage it is useful to directly observe representative equilibrium configurations obtained during GEMC runs. These correspond to particular locations in the phase diagram depicted in Fig. 1b. The results of Fig. 2a-c show strictly equilibrated configurations. Configurations below the microphase transition show slightly irregular domains due to finite temperature entropic fluctuations. For this system, and at the densities and tem-

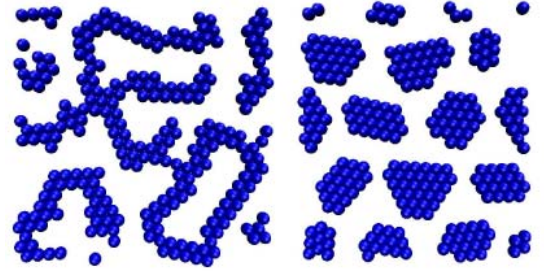


FIG. 3: Left: nearly arrested (gel) configuration at  $t = 5 \times 10^5$  after a rapid quench of the system to  $T_f = 0.08$  with  $\xi = 2$  and  $A = 0.2$  at  $\rho = 0.5$ . Right: equilibrium configuration of the system at  $\rho = 0.5$  and  $T = 0.08$  found by GEMC.

peratures shown, compact cluster states are lower in energy than extended (lamellar) states, which were not observed. The second and third panels illustrating configurations just above and below the microphase line of Fig. 2c are particularly illuminating. Here, such fluctuation effects are particularly strong, even though the transition is first-order. Dynamical behavior upon a rapid quench below the microphase separation line is shown in the first two panels of Fig. 2d [35]. The evolution of the system from the configuration depicted in the second panel to the third panel (equilibrated with GEMC) of Fig. 2d is extremely slow via conventional molecular dynamics.

The dynamical behavior shown in Fig. 2d is clearly relevant for the mechanism of gelation of the system. In particular, consider slightly deeper quench at a lower density than that shown in Fig. 2d. In Fig. 3a a quench of the system is made at  $\rho = 0.5$  to  $T = 0.08$ . After rapid

initial transient dynamics where a tenuous percolating structure is formed, dynamics becomes anomalously slow. This system may be characterized as a gel. Due to the depth of the quench, we did not observe substantial structural coarsening (as is observed in Fig. 2d) over the duration of the simulations, although the energy of the system is slowly evolving in time. Similar evolution is expected to be much slower in the case of a polydisperse, three-dimensional system. For comparison, the equilibrium state of the system (as found via GEMC) is also shown in Fig. 3. Note that the structure of the gel does not resemble the equilibrium state in any regard, despite the fact that the energy per particle in the gel is quite close to that of particles in their cluster ground state. In particular, we find via GEMC no evidence of extended microphase structures at the density and temperature of Fig. 3. Regardless, the short-time critical-like fluctuations that exist during the initial stages of microphase separation are sufficient to generate configurations that span space and evolve anomalously slowly due to strong, short-ranged bonding between particles.

The results presented above are clearly of importance for understanding the general routes to gelation in colloidal systems with competing short-ranged attraction and long-ranged repulsion. We find, rather robustly, that gels may form via arrested *microphase* separation. This is analogous to the purely attractive case, where gels are formed during arrest of global phase separation. This picture is in stark contrast to that of refs [15, 16] where gelation is a consequence of near-equilibrium vitrification of clusters which are stabilized by the repulsive interactions. We have explicitly demonstrated here that, as in the purely attractive case, the gel may be stabilized by the attraction between particles. More interestingly, the gel structure bears no similarity to the clusters that exist in thermodynamic equilibrium. We find that in the system studied here, the only role of the repulsion is the selection of the symmetry of the ground state(s). Our results are fully consistent with, but more general than, the suggestion that disordered configurations of anisotropic microphase structures are connected to gelation [11, 14, 17]. Indeed, we have directly demonstrated that extended microphase structures are not involved during the formation of the gel in Fig. 3. Furthermore, preliminary studies in three dimensions for the system studied in ref. [15] show that for rapid, deep quenches gels may be formed in the same manner even for relatively low ( $\phi \sim 0.15$ ) volume fractions [36]. In general, lamellar and tubular structures (as well as other microphase textures) may comprise the building blocks of the disordered weak solids found in colloidal systems with depletion attractions and long-ranged charge repulsion, but our results demonstrate that they need not. The disordered lamellar and tubular examples are simply some of the many of the ways in which microphase separation may arrest in a manner directly analogous to

the arrest of global phase separation. The collection of all such ways perhaps form the simplest generic route to the gel state at intermediate volume fractions in attractive systems with charge frustration. The search for more exotic routes which may be operative at very low volume fractions and where charge repulsion plays a more active role may be greatly facilitated by the use of the GEMC approach as outlined here.

This work was supported in part by grants NSF-0134969 and FQRNT-91389 (to PC). We would like to thank Dr. E. Del Gado, Prof. D. Frenkel, P. Lu, and Dr. K. Miyazaki for helpful discussions and comments.

---

\* Electronic address: reichman@chem.columbia.edu

- [1] M. E. Cates, M. Fuchs, K. Kroy, W. C. K. Poon, and A. M. Puertas, *J. Phys.: Condens. Matter* **16**, S4861 (2004).
- [2] N. A. M. Verhaegh, D. Asnaghi, H. N. W. Lekkerkerker, M. Giglio, and L. Cipelletti, *Physica A* **242**, 104 (1997).
- [3] S. Manley, H. M. Wyss, K. Miyazaki, J. C. Conrad, V. Trappe, L. J. Kaufman, D. R. Reichman, and D. A. Weitz, *Phys. Rev. Lett.* **95**, 238302 (2005).
- [4] G. Foffi, C. De Michele, F. Sciortino, and P. Tartaglia, *Phys. Rev. Lett.* **94**, 078301 (2005).
- [5] G. Foffi, C. De Michele, F. Sciortino, and P. Tartaglia, *J. Chem. Phys.* **122**, 224903 (2005).
- [6] E. Zaccarelli, S. V. Buldyrev, E. La Nave, A. J. Moreno, I. Saika-Voivod, F. Sciortino, and P. Tartaglia, *Phys. Rev. Lett.* **94**, 218301 (2005).
- [7] E. Del Gado and W. Kob, *Europhys. Lett.* **72**, 1032 (2005).
- [8] S. A. Shah, Y. L. Chen, S. Ramakrishnan, K. S. Schweizer, and C. F. Zukoski, *J. Phys.: Condens. Matter* **15**, 4751 (2003).
- [9] P. N. Segre, V. Prasad, A. B. Schofield, and D. A. Weitz, *Phys. Rev. Lett.* **86**, 6042 (2001).
- [10] S. Mossa, F. Sciortino, P. Tartaglia, and E. Zaccarelli, *Langmuir* **20**, 10756 (2004).
- [11] F. Sciortino, P. Tartaglia, and E. Zaccarelli, *J. Phys. Chem. B* **109**, 21942 (2005).
- [12] R. P. Sear, S. W. Chung, G. Markovich, W. M. Gelbart, and J. R. Heath, *Phys. Rev. E* **59**, R6255 (1999).
- [13] A. Imperio and L. Reatto, *J. Phys.: Condens. Matter* **16**, S3769 (2004).
- [14] A. de Candia, E. Del Gado, A. Fierro, N. Sator, M. Tarzia, and A. Coniglio (2006), cond-mat/0601298.
- [15] F. Sciortino, S. Mossa, E. Zaccarelli, and P. Tartaglia, *Phys. Rev. Lett.* **93**, 055701 (2004).
- [16] J. Wu, Y. Liu, W. R. Chen, J. Cao, and S. H. Chen, *Phys. Rev. E* **70**, 050401(R) (2004).
- [17] M. Tarzia and A. Coniglio, *Phys. Rev. Lett.* **96**, 075702 (2006).
- [18] P. Charbonneau and D. R. Reichman (2006), cond-mat/06XXXX.
- [19] H. Liu, S. Garde, and S. Kumar, *J. Chem. Phys.* **123**, 174505 (2005).
- [20] A. Z. Panagiotopoulos, *Mol. Sim.* **9**, 1 (1992).
- [21] M. G. Noro and D. Frenkel, *J. Chem. Phys.* **113**, 2941 (2000).

[22] D. Frenkel, P. Bladon, P. Bolhuis, and M. Hagen, *Physica B* **228**, 33 (1996).

[23] M. Hasegawa and K. Ohno, *J. Phys.: Condens. Matter* **9**, 3361 (1997).

[24] P. R. ten Wolde and D. Frenkel, *Science* **277**, 1975 (1997).

[25] A. P. Gast, C. K. Hall, and W. B. Russel, *J. Colloid Interface Sci.* **96**, 251 (1983).

[26] M. H. J. Hagen and D. Frenkel, *J. Chem. Phys.* **101**, 4093 (1994).

[27] N. A. Seaton and E. D. Glandt, *J. Chem. Phys.* **84**, 4595 (1986).

[28] M. A. Miller and D. Frenkel, *J. Chem. Phys.* **121**, 535 (2004).

[29] D. Pini, J. L. Ge, A. Parola, and L. Reatto, *Chem. Phys. Lett.* **327**, 209 (2000).

[30] S. A. Brazovskii, *Sov. Phys. JETP* **41**, 85 (1975).

[31] S. Whitelam and P. L. Geissler (2005), *cond-mat/0508100*.

[32] B. Chen and J. I. Siepmann, *J. Phys. Chem. B* **104**, 8725 (2000).

[33] Results are reported in reduced units: temperatures by the well depth  $\epsilon$ , distances by the particle diameter  $\sigma$ , and time by  $(\epsilon/m\sigma^2)^{1/2}$ , where  $m$  is the mass of the particles.

[34] GEMC moves are subdivided between local and non-local moves. At low densities and high temperatures as well as for gas-liquid equilibria both categories are attempted with equal frequency, but in other contexts, non-local moves comprise up to 90% of the attempted moves. Local moves include regular MC single particle displacements (94%), cluster displacements (0.5%), cluster rotations (0.5%), cluster cleaving [31] (0 – 1%), volume exchanges (3%), and asymmetric volume exchanges (1 – 2%) while the non-local moves attempted are particle exchanges (80%), aggregation volume bias [32] (10%), and its generalization to two boxes (10%). In gas-liquid equilibria cluster cleaving are replaced with asymmetric volume exchanges.

[35] Dynamical results are obtained using standard molecular dynamics (MD) integration for systems sizes of at least  $N = 256$ , with an integration step of  $\Delta t = 0.001$ . Cooling is done by velocity resampling every  $10^5$  steps starting initially from a homogeneous fluid configuration. We do not expect a strong influence of the type of dynamics on the qualitative results [5], so further studies with other dynamical protocol are not performed. For computational reasons, the long-ranged repulsive tail is truncated at  $r_c = 5$  for  $\xi = 2$  and at  $r_c = 3.3$  for  $\xi = 1$ . This modification of alters the microphase patterning [13]. However, the results presented here are not sensitive to the form of the ground state for the uncut potential, as comparisons between GEMC and MD simulations are made with consistent values of  $r_c$ .

[36] P. Charbonneau and D. R. Reichman, unpublished.